# Patch-Clamp Characterization of the MscS-like Mechanosensitive Channel from *Silicibacter pomeroyi*

Evgeny Petrov,[†*] Dinesh Palanivelu,[‡] Maryrose Constantine,[†] Paul R. Rohde,[†] Charles D. Cox,[††] Takeshi Nomura,[†] Daniel L. Minor, Jr.,[‡§¶‖‡‡] and Boris Martinac[†§§*]

[†]Victor Chang Cardiac Research Institute, Darlinghurst, Australia; [‡]Cardiovascular Research Institute, [§]Department of Biochemistry and Biophysics, [¶]Department of Cellular and Molecular Pharmacology, and [‖]California Institute for Quantitative Biomedical Research, University of California, San Francisco, California; [††]School of Pharmacy and Pharmaceutical Sciences, Cardiff University, Cardiff, UK; [‡‡]Physical Biosciences Division, Lawrence Berkeley National Laboratories, Berkeley, California; and [§§]St. Vincent's Clinical School, University of New South Wales, Sydney, Australia

ABSTRACT Based on sequence similarity, the sp7 gene product, MscSP, of the sulfur-compound-decomposing Gram-negative marine bacterium *Silicibacter pomeroyi* belongs to the family of MscS-type mechanosensitive channels. To investigate MscSP channel properties, we measured its response to membrane tension using the patch-clamp technique on either a heterologous expression system using giant spheroplasts of MJF465 *Escherichia coli* strain (devoid of mechanosensitive channels MscL, MscS, and MscK), or on purified MscSP protein reconstituted in azolectin liposomes. These experiments showed typical pressure-dependent gating properties of a stretch-activated channel with a current/voltage plot indicating a rectifying behavior and weak preference for anions similar to the MscS channel of *E. coli*. However, the MscSP channel exhibited functional differences with respect to conductance and desensitization behavior, with the most striking difference between the two channels being the lack of inactivation in MscSP compared with MscS. This seems to result from the fact that although MscSP has a Gly in an equivalent position to MscS (G113), a position that is critical for inactivation, MscSP has a Glu residue instead of an Asn in a position that was recently shown to allosterically influence MscS inactivation, N117. To our knowledge, this study describes the first electrophysiological characterization of an MscS-like channel from a marine bacterium belonging to sulfur-degrading $\alpha$-proteobacteria.

## INTRODUCTION

MscS was the first bacterial mechanosensitive (MS) channel to be examined by means of the patch-clamp technique (1). Since the cloning of the *mscS* gene (2), MscS has emerged as the prototype of a diverse family of MS channels found in bacteria, archaea, fungi, and plants (3,4). The physiological function of MscS can clearly be correlated with its structural and electrophysiological properties. Bacteria exposed to distilled water (osmotic downshock) rapidly release cytoplasmic contents into the surrounding medium, indicating that MscS functions as an osmotically activated emergency valve. The *Escherichia coli* double-knockout strains *ΔmscL* and *ΔmscS*, which are devoid of the two highest-conducting MS channels, were found to lyse upon a mild osmotic shock (2). Mutation studies established that gain-of-function (GOF) mutants with leaky MscS channels are less viable or can hardly grow (5). The availability of the MscS crystal structure (6,7) allows for detailed structure and function studies, as well as investigations of lipid bilayer effects on gating of this channel (8–12).

From an evolutionary perspective, the MscS channel subfamily provides a rich source for studies of the molecular evolution of these membrane proteins from their basic function as cellular osmosensors to more specialized but as yet unknown cellular tasks. The availability of MscS-type and other MS channel proteins in prokaryotic cells makes them suitable for overexpression in *E. coli* for structural characterization by x-ray crystallography (6,7,13) and/or electron paramagnetic resonance spectroscopy (11). The secondary structure of MscS variants found in different organisms is highly diverse. For example, MscS from *E. coli* has three transmembrane (TM) helices (2), whereas MscCG, the MscS variant found in the Gram-positive soil bacterium *Corynebacterium glutamicum*, has four (14). MscS variants within extremophiles possess three to five TM helices (15), and in the plant *A. thaliana* the range is from three to six helices (16).

In this study, we used the patch-clamp technique to investigate the functional properties of an MscS-like membrane protein from the extremophilic bacterium *Silicibacter pomeroyi*. We call this membrane protein MscSP in accordance with the terminology for other prokaryotic members of the MscS family. MscSP has good expression properties (15) and a high degree of structural homology to *E. coli* MscS (Fig. 1). MscSP was successfully expressed and purified from *E. coli* for reconstitution into azolectin liposomes, and was also expressed in the triple-knockout *E. coli* strain MJF465 (lacking three major MS channels: MscL, MscS, and MscK) to form giant spheroplasts suitable for direct patch-clamping. Patch-clamp recordings from membrane patches of giant spheroplasts, as well as proteoliposomes, showed that MscSP responded to membrane tension and displayed activity characteristic of an MscS-like channel. To

*Submitted August 25, 2012, and accepted for publication January 14, 2013.*

*Correspondence: b.martinac@victrochang.edu.au or petrov67@gmail.com

Editor: Jose Faraldo-Gomez.



0006-3495/13/04/1426/9

http://dx.doi.org/10.1016/j.bpj.2013.01.055

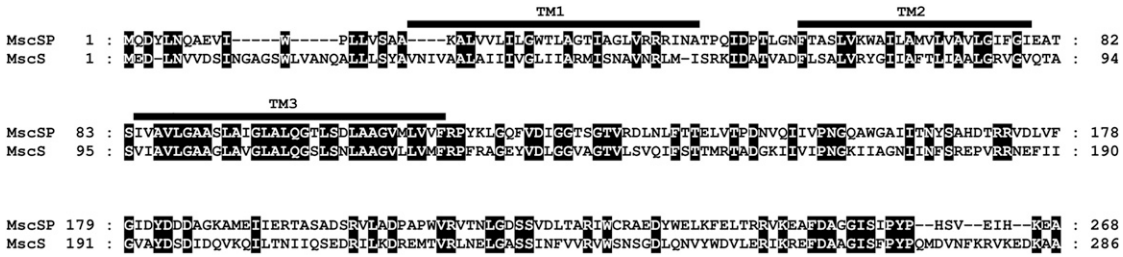


FIGURE 1 MscSP versus MscS sequence alignment. Comparison of the primary amino acid sequence between MscS of *E. coli* and its homolog from *S. pomeroyi*, MscSP. The alignment reveals ~40% sequence identity. Identical residues are marked with a black box and TM domains (6) TM1, TM2, and TM3 are represented by black bars.

our knowledge, this study presents the first electrophysiological characterization of this MscS homolog, which is the first homolog to be identified in marine bacteria, $\alpha$-proteobacteria, and sulfur-compound-decomposing bacteria.

## MATERIALS AND METHODS

### Plasmids

Two different constructs of wild-type (WT) MscSP were generated for spheroplast production and protein purification. For protein expression, the pQE-30 plasmid (Qiagen, Germantown, MD) incorporated the coding sequence for WT MscSP with an N-terminal 6-His tag and thrombin cleavage site. For spheroplast expression, the pQE-60 (Qiagen) contained the coding sequence for WT MscSP. Previously, the pQE-60 plasmid had the lacI coding region from pREP4 (Qiagen) inserted into a blunted NdeI site. The plasmids were constructed as follows:

1. The sequence for MscSP was amplified by polymerase chain reaction (PCR) from the MscSP template DNA using the primers ATTCGAGGTCTCCCATGCAGGACTATCTGAACCAG and TAAGG GATCCTTAGGCCTCCTTGTGGATCTCGAC. The PCR product was digested with Bsa I and Bam HI and then ligated into pQE-60 lacI previously digested with NcoI and BamHI.

This construct was for spheroplast production only, as no hexahistidine purification tag is present.

2. For the PQE-30 MscSP construct, the sequence for MscSP was amplified by PCR from pQE-60 lacI MscSP using the primers ATTGGC ATGCCTGGTTCCGCGTGGACCTATGCAGGACTATCTGAACCAG and TAAGAAGCTTTTAGCCGGCCTCCTTGTG. The PCR product and pQE-30 were both digested by *Hin*dIII and SphI and then ligated.

### Giant spheroplast preparation

Giant spheroplasts were generated from MJF465 *E. coli* transformed with the pQE-60 lacI MscSP plasmid, with some modifications to the originally described method (1). A single colony was selected and incubated overnight in lysogeny broth (LB) media with 100 $\mu$g/ml ampicillin, 12.5 $\mu$g/ml kanamycin, and 12.5 $\mu$g/ml chloramphenicol at 37°C (180 rpm). The overnight culture was diluted 1:100 in LB media containing the aforementioned antibiotics and incubated at 37°C (180 rpm). Once an $OD_{600}$ of 0.4 was reached, this culture was diluted 1:10 in LB media with 60 $\mu$g/ml cephalexin.

The culture was incubated at 37°C (120 rpm) until the single-cell filaments reached 50–150 $\mu$m in length (~90 min), and then was induced with 0.5 mM isopropyl $\beta$-D-1-thiogalactopyranoside (IPTG) and further incubated for 75 min at 18°C, 150 rpm. The filaments were harvested by centrifugation (1500×*g*, 5 min, 4°C) and the pellet was resuspended gently in 2.5 ml of 0.8 M sucrose. Then 150 $\mu$l of 1 M TrisCl (pH 7.2), 120 $\mu$l of lysozyme (5 mg/ml), 30 $\mu$l of DNase (5 mg/ml), and 120 $\mu$l of 0.125 M EDTA (pH 8.0) were mixed sequentially to the mixture. The mixture was incubated at room temperature for 3–7 min to allow the peptidoglycan layer to be hydrolyzed, and spheroplast formation was monitored under the microscope. Once spheroplasts were formed, 1 ml of stop solution (1 M $MgCl_2$, 0.8 M sucrose, and 1 M Tris Cl, pH 7.2) was added immediately and mixed. The mixture was incubated at room temperature for 5 min and then the culture tubes were transferred to ice and 7 ml of cushion solution (10 mM $MgCl_2$, 0.8 M sucrose, and 10 mM TrisCl, pH 7.2) was layered over each pellet. The suspension was centrifuged at 1000×*g* for 2 min and then the supernatant was carefully aspirated, leaving only 300 $\mu$l. The sample was then examined under the microscope; if the spheroplasts appeared to be too concentrated, the sample was diluted with cushion solution and then aliquoted and stored at −20°C.

### Purification of MscSP protein

Competent M15 *E. coli* cells containing pREP4 (Qiagen) and pRARE (Merck) were transformed with the pQE-30 (Qiagen) MscSP fusion expression plasmid. Cells were cultured in 2YT media with the appropriate antibiotics (ampicillin 100 $\mu$g/ml, kanamycin 12.5 $\mu$g/ml, and chloramphenicol 12.5 $\mu$g/ml) at 37°C. Once an OD600 of 0.6 was reached, cells were induced by the addition of 0.8 mM IPTG in the presence of 0.4% glycerol and incubated for 24 h at 18°C. Cells were harvested (3000×*g*, 10 min, 4°C) and resuspended in Tris HCl pH 7.5 (10 ml per gram of pellet). Then 200 $\mu$g/ml phenylmethanesulfonylfluoride (PMSF; Roche) and ~1 mg DNaseI (DN25; Sigma-Aldrich, St. Louis, MO) were added to the suspension before the cells were disrupted twice via a French press (16,000 psi; Thermo Scientific (Thermo Fisher Scientific Australia Pty Ltd, Scoresby Vic) ). Lysates were centrifuged to remove cell debris (12,000×*g*, 15 min, 4°C) and then membranes were collected/extracted (235,000×*g*, 2 h, 4°C) and solubilized overnight with mixing at 4°C in 50 mM Tris HCl buffer containing 8 mM n-dodecyl-β-D-maltoside (DDM) (cat. No. D310; Anatrace, Maumee, OH), 10% glycerol, and 97 $\mu$M PMSF. After clarification (105,000×*g*, 20 min, 4°C), the MscSP fusion protein was purified via immobilized metal affinity chromatography using TALON (Clontech, Mountain View, CA) $Co^{2+}$ sepharose. The column was washed sequentially with buffer 1 (50 mM Tris HCl pH 7.5, 1 mM DDM, and 10% glycerol), followed by buffer 2 (50 mM Tris HCl pH 8 with 5 mM imidazole, 1 mM DDM, and 10% glycerol) and again with buffer 1 (50 mM Tris HCl, pH 7.5, containing 1 mM DDM and 10% glycerol (10× resin volume)). The resin was resuspended with an equivalent amount of the aforementioned buffer 1 and cleaved with 20 U thrombin (GE Amersham) per milligram of solubilized membranes with mixing for 4 h at room temperature (25°C), and then overnight at 4°C. Alternatively, the protein was eluted without cleavage using buffer containing 50 mM Tris HCl pH 8, 300 mM imidazole, 1 mM DDM, and 10% glycerol (10× resin volume).

Imidazole was removed by washing the sample twice through an Amicon Ultra 15 Centrifugal Device (100 kDa; Millipore, Billerica, MA) with buffer 1 (50 mM Tris HCl pH 7.5 containing 1 mM DDM and 10% glycerol). The protein was collected and stored at 4°C. The yield of WT MscSP was 0.92 mg/ml per liter of 2YT culture. The functionality of the protein was verified by patch-clamping.

## Liposome preparation and MscSP reconstitution

### *Dehydration-rehydration method*

Soybean azolectin was purchased from Sigma-Aldrich and used without further purification. The method we used was adapted from one described by Häse et al. (17). Briefly, 10 mg of lipid was dissolved in chloroform and then air-dried under a stream of $N_2$ gas. To this we added 1 ml of the dehydration-rehydration (D/R) solution containing 200 mM KCl and 5 mM HEPES (pH adjusted to 7.2 using KOH). The resulting suspension was sonicated for 20 min. Then 200 $\mu$l (2 mg lipid total) was taken from this solution and put into a 10 ml falcon tube, and the appropriate volumes of MscL and MscSP were added to achieve a protein/lipid ratio of 1:1000 w/w for MscL and 1:100 w/w for MscSP, respectively. The resulting suspension was sonicated for 20 min. Then 200 $\mu$l (2 mg lipid total) was taken from this solution and put into a 15 ml falcon tube, and the appropriate volume of MscL was added to achieve a protein/lipid ratio of 1:1000 w/w. The volume was increased to 3 mL using the bulk solution above and the tube was placed on a rotary wheel for 1 h. Bio-Beads (SM-2; BioRad, Richmond, CA) were then added and the solution was further rotated for another 3 h. After this time, the solution was centrifuged at 40,000 rpm ($\approx$193,000$\times g$) for 30 min. The pellet was collected, spotted onto a microscope slide, and dehydrated under vacuum overnight at 4°C. The dried lipid spot was then rehydrated with a 40 $\mu$l drop of D/R solution and kept at 4°C for 24 h.

## Sucrose method

As an alternative method, we also used the sucrose method as previously described by Battle and Martinac (18). Briefly, we dissolved 10 mg of soybean azolectin in 1 ml of chloroform and then put a 200 $\mu$l aliquot into a 12×75 mm test tube. We evaporated the solvent with a stream of dry $N_2$ while shaking and rotating the tube. Next, we put 2 $\mu$l of distilled water into the bottom of the tube as a prehydration step. After 5 min, we put 1 ml of 0.4 M sucrose into the bottom of the tube (rehydration step). The tube was closed with plastic foil and placed in a preheated oven at 55°C for 3 h. An aliquot of the MscSP protein was added to the bottom of the tube and the tube was placed vertically on an orbital shaker with shaking overnight at 140 rpm at room temperature. By the next morning, the lipids had formed a floating cloud to which 0.5 $cm^3$ of Bio-Beads (BioRad) was added to absorb the detergent.

## Patch-clamp recording from giant MJF465 *E. coli* spheroplasts and azolectin liposomes

An aliquot (1.5–3 $\mu$l) of giant spheroplasts or an aliquot (2–4 $\mu$l) from the rehydrated liposomes was taken and added to the recording bath. We examined MscSP channel activity using the patch-clamp method with the inside-out configuration in giant spheroplasts that were caught floating above the bottom of the recording chamber (1) or on liposomes that settled on the bottom of the recording chamber and formed unilamellar blisters (19). The spheroplasts were placed in a bath containing (unless otherwise stated) 250 mM KCl, 90 mM $MgCl_2$, and 5 mM HEPES (pH 7.2), whereas proteoliposomes were placed in the recording chamber containing 200 mM KCl, 40 mM $MgCl_2$, 5 mM HEPES (pH 7.2). Negative pressure (suction) recorded in mm Hg was applied to patch pipettes with a syringe and monitored with the use of a piezoelectric pressure transducer (Omega Engineering, Stamford, CT). Borosilicate glass pipettes (Drummond Scientific, Broomall, PA) were pulled using a Flaming/Brown pipette puller (P-87; Sutter Instrument, Novato, CA) to a diameter that corresponded to a pipette resistance in the range of 3.5–5.1 MΩ. Ion currents that arose from activation of MscL were recorded with an Axon 1D patch-clamp amplifier (Axon Instruments, Molecular Devices, Sunnyvale, CA), filtered at 2 kHz, and digitized at 5 kHz. Single-channel analysis was done using pCLAMP10 software (Axon Instruments). Bath and pipette solutions were symmetrical and consisted of 200 mM KCl, 40 mM $MgCl_2$, 5 mM HEPES (solution adjusted to pH 7.2 using KOH).

# RESULTS

## Structural similarities and differences between MscSP and MscS

A pairwise alignment of the amino acid sequence of MscS and its *S. pomeroyi* homolog MscSP revealed a high degree of sequence conservation, showing ~40% identity between the two protein sequences (Fig. 1) (20). MscSP is a 29 kDa protein consisting of 268 residues, and thus it is 18 residues shorter than MscS, which consists of 286 amino acids (2). This is due to a shorter N- terminus and apparently a smaller C-terminal domain of MscSP compared with MscS (Fig. 2). Like MscS (6), MscSP has three predicted TM domains (15): TM1, TM2, and TM3, which exhibit the highest level of homology with MscS (Fig. 2). In particular, the putative TM3 helix of MscSP shows >95% sequence similarity to that of MscS. A homology model of MscSP based on the crystal structure of an open form of MscS (PDB: 2VV5) (21) created using the Swiss-Model program illustrates this point further. A number of residues that are critical for MscS functionality are conserved in MscSP, including the corresponding residues to 1), F68 and L111, which are involved in tension sensing and inactivation; 2), L105 and L109, which in MscS form a hydrophobic lock that prevents ion permeation; 3), G113, which is critical for inactivation; and 4), a number of residues that have been shown to be important for the mechanosensing of MscS (Fig. 2). Based on the high level of its sequence similarity to MscS, MscSP appeared to be an excellent example of a membrane protein that would be expected to exhibit the properties of an MS channel.

## Patch-clamp analysis from MscSP of *S. pomeroyi*

We investigated the mechanosensitivity of MscSP using the patch clamp in giant spheroplasts of *E. coli* carrying *mscSP* plasmid or upon reconstitution of purified protein into azolectin liposomes (Fig. 3; Materials and Methods). MscSP channels reconstituted into liposomes could be activated by negative pressure applied to patch pipettes in the range of −20 to −30 mmHg, similarly to the MscS channels, whereas in membrane patches of giant spheroplasts the range of negative pressures that activated MscSP varied between −100 and −130 mm Hg (Fig. 4). Given that the diameter and shape of the patch pipettes in our experiments

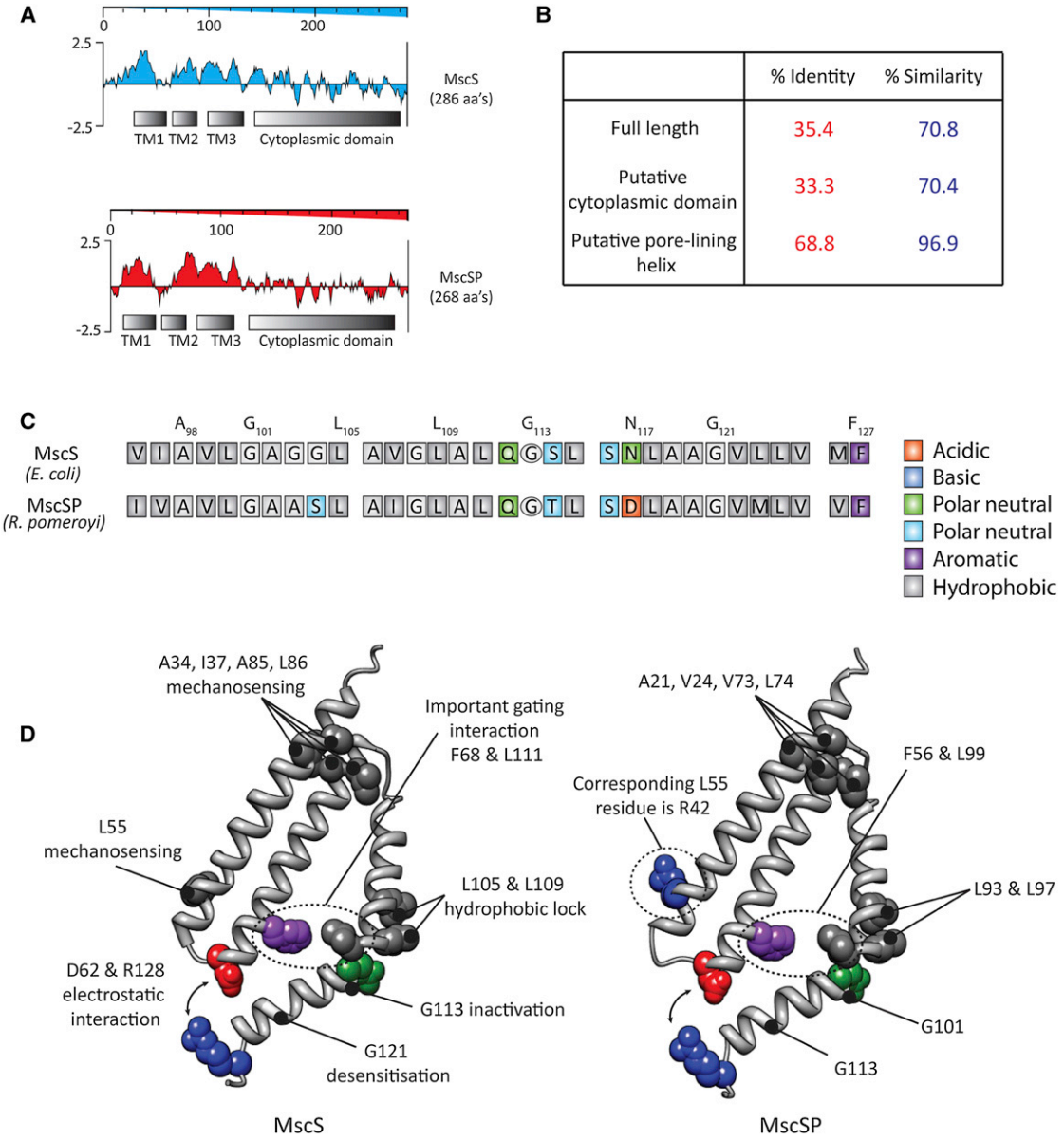


FIGURE 2 Comparison of MscS and MscSP structures. (*A*) Corresponding hydropathy plots for MscS and MscSP were determined using the Kyte-Doolittle algorithm. Gray bars beneath represent the respective TM helices and cytoplasmic domains. (*B*) Pairwise alignment of MscS with MscSP showing percentage identity and similarity of the full-length proteins, cytoplasmic domains, and pore-forming helices. (*C*) Pairwise sequence alignment of the MscS pore-forming helix and the putative pore-forming helix of MscSP further illustrates the high level of similarity between these homologs. (*D*) Comparison of a homology model of MscSP created using the Swiss-Model program with the structure of MscS (PDB: 2VV5). Important functional residues in MscS are highlighted on the left and their corresponding residues in MscSP are shown on the right.

were nearly constant, as evidenced by the bubble number of 3.8–4.6 (22) and pipette resistance of 3.5–5.1 MΩ, the higher pressure needed for activation of MscSP channels recorded in giant spheroplasts compared with MscSP reconstituted into liposomes most likely resulted from extrinsic factors such as remnants of the peptidoglycan cell wall in spheroplast patches, as was previously shown for MscS and MscL (19,23). The previously reported pressures required for activation of MscS recorded in *E. coli* giant spheroplasts using standardized patch pipettes varied between −30 and −70 mm Hg (19). Overall, the range of MscSP activation pressures in this study is below or comparable to the pressure required for activation of MscL (Table 1; Fig. 4) (24,25). It was also previously reported that increasing pipette pressure (and hence membrane tension) results in successive opening of the MscS and MscL channels (26), and the MscL/MscS pressure activation ratio has been defined as a determining factor in bacterial cells' response to hypoosmotic shock (19,27). Thus, to obtain a measure of MscSP's mechanosensitivity relative to that

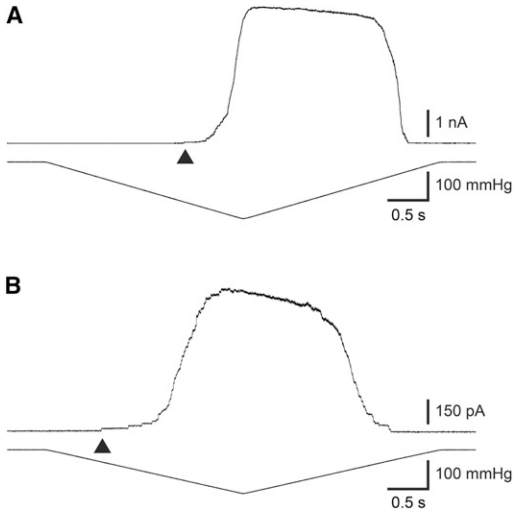


FIGURE 3 Activation of MscSP by membrane tension. MscSP protein was successfully expressed in the native *E. coli* membrane and reconstituted into liposome bilayers. (*A* and *B*) In both cases, MscSP exhibited activities of a functional MS channel: (*A*) giant spheroplasts and (*B*) azolectin liposomes. The activity of tens of active channels could be recorded in both preparations. Arrowheads point to the first channel opening observed in the current traces shown.

of MscL, we coreconstituted it together with MscL into liposomes (Fig. 5). We determined the MscL/MscSP ratio to be 1.28 ± 0.08 ($n = 7$; Table 2), which is significantly smaller than the MscL/MscS ratio reported previously (2.00 ± 0.12, $n = 4$; Table 2 (19)). This indicates that MscSP requires a higher membrane tension for activation than MscS (see Discussion).

The Boltzmann distribution function describing the open probability, $P_o$, plotted versus negative pipette pressure for MscSP is shown in Fig. 4 *A*. Overall, MscSP recorded in liposome patches required more pressure for activation, as reflected by its midpoint activation value of $p_{1/2} = -54.63 \pm 2.72$, compared with MscS, whose midpoint activation ratio was –35.26 ± 2.00 (Table 1). As was previously shown (23), the product of the midpoint activation pressure $p_{1/2}$ and $\alpha$, which is the slope of the plot ln $[P_o/(1 - P_o)]$ versus pressure and thus the inverse of the pressure required for an e-fold change in the channel $P_o$, provides a direct estimate of the energy difference $\Delta G_0$ between the closed and open states of an MS channel. It is characteristic of any type of MS channel that has been reconstituted into a defined liposome membrane. For MscSP we determined a $\Delta G_0$ of 12.6 ± 1.2 kT ($n = 7$) (in azolectin) and 20.6 ± 1.8 kT ($n = 7$) (in spheroplast membrane), whereas for MscS $\Delta G_0$ in liposomes was 17.3 ± 1.0 ($n = 5$). Interestingly, unlike MscS (28,29), MscSP does not desensitize with the channels remaining open for up to 3 min at constant membrane tension (Fig. 5 *B*). This is similar to what was reported for MscCG, the MscS-like channels from the soil bacterium *Corynebacterium glutamicum* (14), as well as for MscMJ and MscMJLR,

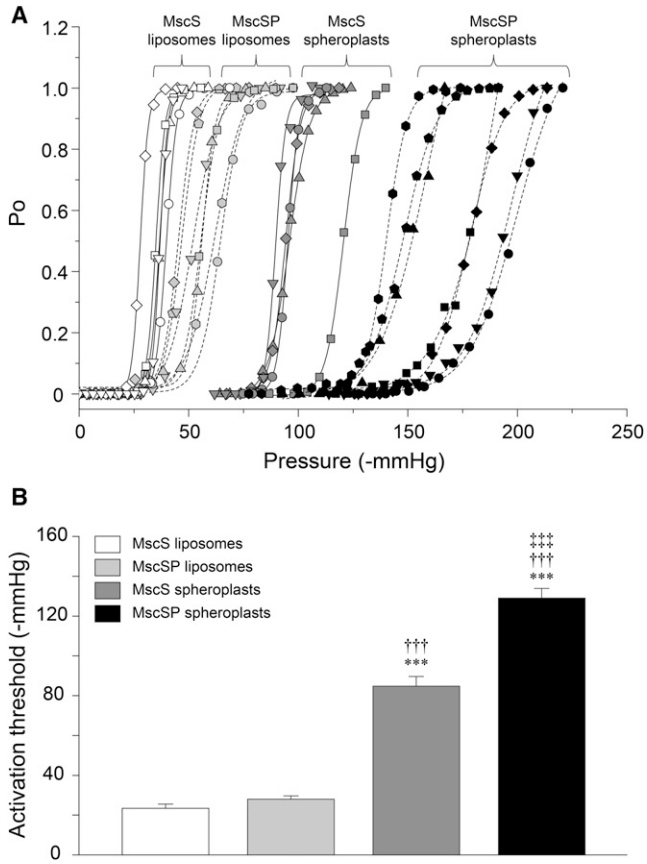


FIGURE 4 Boltzmann distribution curves for MscSP and MscS. (*A*) Mechanosensitivity profile plotted as a function of open probability $P_o$ and negative pressure. $P_o$-values for MscS reconstituted into azolectin liposomes (*open symbols*), for MscSP reconstituted into azolectin liposomes (*solid symbols*; Boltzmann curves on the left), and for MscS (*gray symbols*) and MscSP (*black symbols*) in spheroplast membrane, respectively (Boltzmann curves on the right), are shown with their best-fit plots as indicated in the figure above each set of Boltzmann curves. Note the similarity in mechanosensitivity between MscS and MscSP in azolectin liposomes, and the small difference between MscSP in azolectin and MscSP in spheroplast membrane. (*B*) Activation threshold of MscS and MscSP reconstituted into azolectin liposomes and MscSP expressed in spheroplasts, respectively. The asterisk, dagger, and double dagger indicate that the value is significantly different from MscS and MscSP reconstituted into liposomes, respectively (***$p < 0.001$ vs. MscS liposomes, $^{\dagger\dagger\dagger}p < 0.001$ vs. MscSP liposomes, $^{\ddagger\ddagger\ddagger}p < 0.001$ vs. MscS spheroplasts by *t*-test); *n* indicates the number of different patches tested. All values are represented as mean ± SE.

the MscS-like channels from the archaeon *Methanococcus jannashii* (30).

As with MscS, the MscSP channels strongly rectify (Fig. 6 *C*). Its unitary conductance at positive voltages is 1.04 ± 0.03 nS ($n = 8$) and 0.61 ± 0.02 nS ($n = 8$) at negative voltages in symmetric 250 mM KCl, 90 mM $MgCl_2$ liposome recording solution (see Materials and Methods). The strong rectifying properties of MscSP are indicated by the conductance at negative pipette voltages being approximately two-thirds of the conductance at positive voltages. This closely resembles the behavior of *E. coli* MscS, whose conductance was measured to be 0.82 ± 0.02 nS at negative pipette

**TABLE 1 Midpoint activation pressure of reconstituted MscS, MscSP, and MscL channels in liposome patches**

| Midpoint activation pressure | | | | | |
|---|---|---|---|---|---|
| MscS (mmHg) | *n* | MscSP (mmHg) | *n* | MscL (mmHg) | *n* |
| –35.26 ± 2.00 | 5 | –54.63 ± 2.72* | 7 | –71.42 ±2.22*† | 5 |

Results were obtained from MscS, MscSP, and MscL channels reconstituted into azolectin (100%) liposomes. The asterisk and dagger indicate significantly different values compared with MscS and MscSP (*$p < 0.01$, †$p < 0.01$ by *t*-test), respectively; *n* indicates the number of liposome patches tested. All values are represented as mean ± SE.

**TABLE 2 Midpoint activation ratio and threshold activation ratio of the reconstituted or coreconstituted MscS, MscSP, and MscL channels in liposome patches**

| Midpoint activation ratio | | Threshold activation ratio | | | |
|---|---|---|---|---|---|
| (reconstituted) | | (coreconstituted) | | | |
| MscL/MscS | MscL/MscSP | MscL/MscS | *n* | MscL/MscSP | *n* |
| 2.03 | 1.31 | 2.00 ± 0.12 | 4 | 1.28 ± 0.08* | 7 |

Results were obtained from MscS, MscSP, and MscL channels reconstituted or coreconstituted into azolectin (100%) liposomes. The midpoint activation ratio was calculated using the values for midpoint activation ratio from Table 1. The threshold activation ratio of MscL/MscS was adopted from Nomura et al. (19). The asterisk indicates that the value of MscL/MscSP is significantly different from the value of MscL/MscS (*$p < 0.05$ by *t*-test); *n* indicates the number of liposome patches tested. All values are represented as mean ± SE.

voltages and 1.37 ± 0.05 nS at positive voltages, and thus it is also about two-thirds of that obtained at positive pipette voltages as previously reported (1) Furthermore, in comparison with MscS, the MscSP channel exhibits at least one prominent and several minor substates near the fully open state (Fig. 6, *A* and *B*). Also, like MscS, MscSP exhibits a weak preference for anions ($P_{Cl}/P_K$ = ~1.4; Fig. 7 *A*).

## DISCUSSION

We used patch-clamp analysis to examine the mechanosensitivity of the MscSP membrane protein from *S. pomeroyi* expressed in an *E. coli* mutant lacking all MS channels of the MscL, MscS, and MscK types. Based on amino acid sequence similarity, MscSP is a member of the MscS family of MS channels (3,4,16). As expected, the MscSP channels exhibited the typical pressure-dependent gating behavior of stretch-activated channels, with a current/voltage dependence indicating rectifying behavior comparable to that of MscS (1). The way the channel rectifies is indicated by larger conductance at positive pipette voltages compared with that at negative pipette voltages, which is comparable to the way MscS rectifies (Fig. 6 *C*) (1,8). MscS rectification has been suggested to result at least in part from some conformational change in the protein due to a switch in the direction of the electric field (28). However, we believe that it results largely from the right-side-out orientation of the channels in inside-out spheroplast patches of giant bacterial spheroplasts, meaning that the periplasmic (extracellular) side of MscSP is facing the interior of the patch pipettes, whereas the cytoplasmic C-terminal portion is facing the bath solution (1) (Nomura, T. and Martinac, B., unpublished). In Fig. 6 *C*, I-V curves for both MscS and MscSP channels are plotted against the pipette voltage, which takes into account the fact that different laboratories might use different conventions, such as plotting the I-V curves against membrane potential rather than the pipette voltage (1,8,31,32). Furthermore, the ion selectivity of MscSP is comparable to that of MscS ($P_{Cl}/P_K$ ~1.5–3.0) (1,8), showing a similarly weak preference for anions ($P_{Cl}/P_K$ = ~1.4). The slight preference of MscSP for anions is compatible with the charge distribution inside the cytoplasmically located C-terminal domain of the channel (Figs. 1 and 7 *B*) (31,33,34). However, in comparison with MscS from *E. coli*, the MscSP channel was found to exhibit some differences.

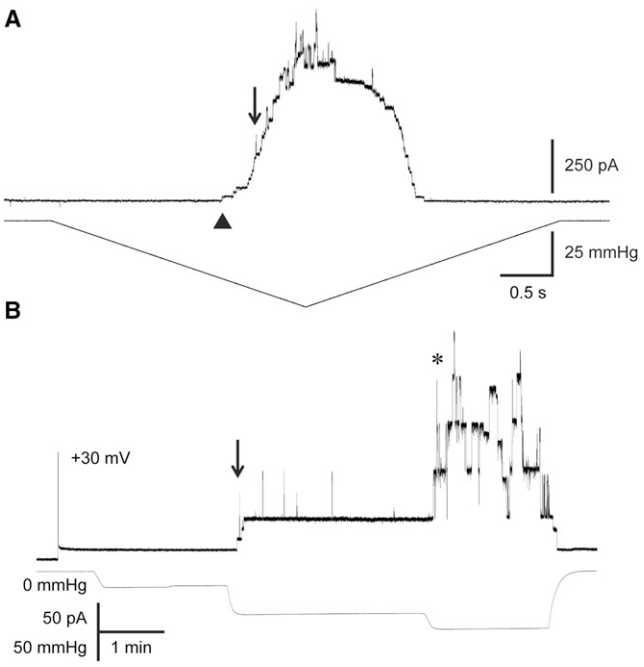


FIGURE 5 MscSP and MscL channels coreconstituted into azolectin liposomes. (*A*) Channel activities of MscS and MscL upon activation by a pressure ramp in azolectin liposomes. The arrowhead and arrow indicate the first opening of MscSP and MscL, respectively. The pipette potential was +30 mV. (*B*) Current (*upper*) trace shows opening of three MscSP (arrow) and four MscL (*) channels upon activation by pressure steps. Note that MscSP channels have a lower opening threshold than MscL and do not desensitize like MscS (see Discussion). The lower trace shows negative pressure applied to the patch electrode. The voltage applied to the patch pipette is shown in the upper-left corner, and the pressure-current timescale is shown in the bottom-left corner.

MscSP has a smaller conductance than MscS from *E. coli* (~25% smaller at both positive and negative pipette voltages). In addition, unlike MscS, MscSP does not desensitize/inactivate, similarly to MscCG of *C. glutamicum* (35) and MscMJ and MscMJLR of *M. jannashii* (30). The

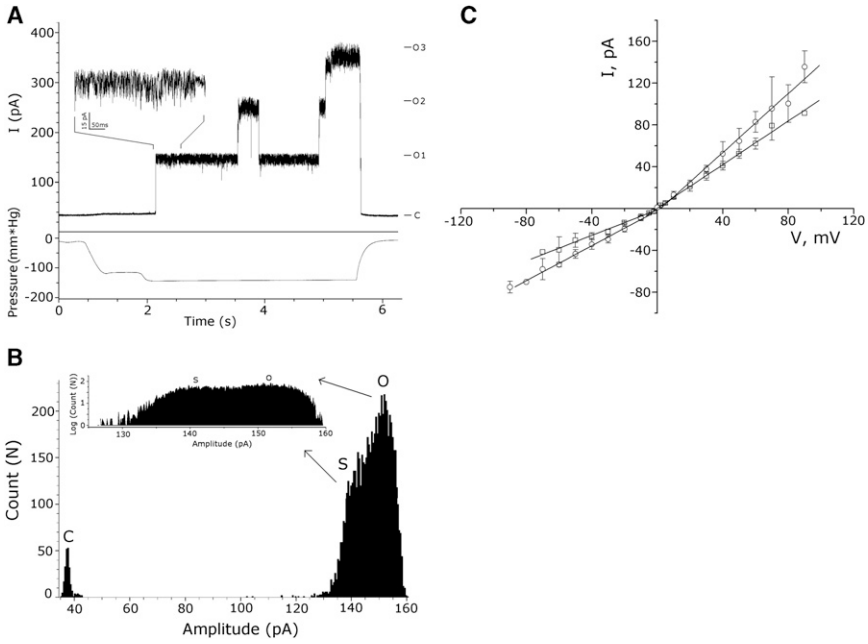


FIGURE 6 Single-channel activity and current-voltage plots for MscSP and MscS. (*A*) Substates of MscSP. Three channels are active in the patch. The inset shows a scaled fragment of the open state of one channel (at +50 mV). (*B*) Amplitude histogram shows several substates near the open state. The inset shows the same histogram, with N shown on the logarithmic scale. Note the single substate (S) and multiple substates between S and the open state (O). (*C*) Current-voltage plots show the single-channel conductance of MscSP (□) and MscS (○) (see Results).

channels remained open for several minutes in response to prolonged application of membrane tension (data not shown). This is interesting because MscSP has a conserved glycine residue at the equivalent position to G113 in MscS. This residue is purported to be the center of inactivation where a kink in the TM3 helix prevents a hydrophobic interaction between F68 from TM2 and both L111 and L115 of the TM3 helix (Fig. 2). In MscS there is also an important interaction between the TM3b helix (N117) and the cytoplasmic domain (G168) during inactivation that promotes the kink around G113. Introduction of a charged residue here prevents MscS inactivation (37). The fact that alignments of MscS and MscSP show N117 replacement for a Glu residue may explain why MscSP does not display inactivation while still possessing an equivalent glycine to G113 in MscS. The loss of this TM3b interaction with the cytoplasmic domain, as well as replacement of Gly113 with amino acids of higher helical propensity (e.g., Glu, Ser, and Asp in MscK of *E. coli*, MscCG of *C. glutamicum*, and MscMJ of *M. jannashii*, respectively (Cox D.D., Nomura, T., Ziegler, C.S., Campbell, A.K., Wann, K.T., and Martinac, B., unpublished)) likely accounts for the lack of inactivation seen in these MscS homologs. Thus, the desensitization described in MscS does not appear to be a core feature of the MscS family (38). MscSP activated at higher tension in membrane patches of giant spheroplasts characterized by 8.7 ± 0.8 mm Hg ($1/\alpha$) per e-fold change in the channel activity and midpoint activation pressure $p_{1/2}$ of 171.9 ± 8.9 mm Hg, compared with $1/\alpha = -4.6 \pm 0.5$ mm Hg in liposome patches and midpoint of activation pressure of $p_{1/2} = -54.6 \pm 2.7$ (Fig. 4 and Table 1). This is comparable to MscS and MscL, which depending on the type of lipids involved exhibit increased mechanosensitivity in liposome patches compared with giant spheroplasts (19). As shown here for MscSP, the increase in their mechanosensitivity is largely characterized by a parallel shift on the pressure (membrane tension) axis of their corresponding Boltzmann distribution functions

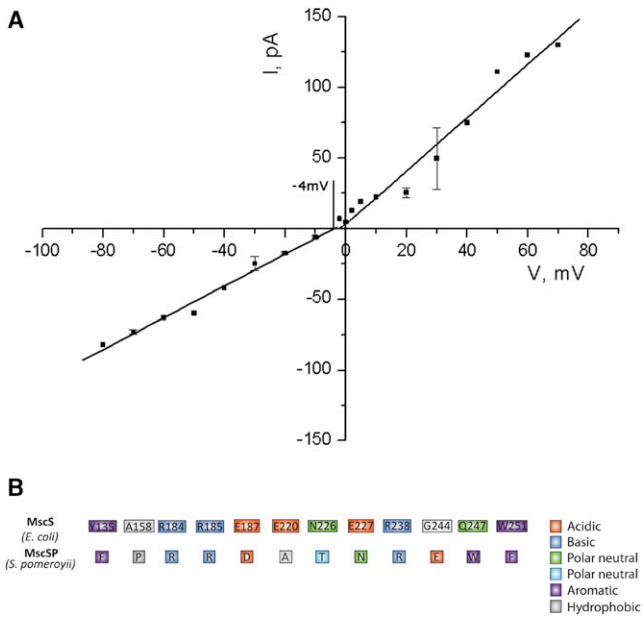


FIGURE 7 Ion selectivity of MscSP. (*A*) Current-voltage plot of the MscSP single channel recorded in high potassium (750 mM KCl) bath solution. The reversal potential is ~−4 mV. This is an indication of weak preference of MscSP channel for $Cl^-$ ions. (*B*) Sequence alignment of vestibular portal residues of MscS and MscSP are shown for comparison. The residues circled are those contributing to weak anionic selectivity in MscS.

toward lower pressure (tension) (8,39). The small difference in slope of the Boltzmann curve for MscSP in spheroplasts compared with liposome membrane patches may be a result of MscSP's interaction with various membrane components in the native spheroplast membrane, since it has been reported that coclustering with MscL affects the pressure sensitivity of MscS (19).

When suspended in a hypotonic medium, marine bacteria lyse but can be rescued from lysis by the presence of $\geq$200 mM NaCl or KCl, with NaCl being much more effective in preventing cell lysis (12). This suggests that marine and in particular halophilic bacteria may not necessarily need to be fully equipped with various types of MS channels, as is the case, for example, for *E. coli*. Indeed, the slightly halophilic marine bacterium *Vibrio alginolyticus* is sensitive to osmotic stress and lyses under osmotic downshock although it has other MS MscS-like channels of smaller conductance. However, Nakamaru et al. (40) were able to rescue it from lysis under hypoosmotic conditions by introducing an *mscL* gene into it. In contrast, as a marine bacterium adaptable to environments of different salinity, *S. pomeroyi* is well equipped with MS channels because it harbors both MscS- and MscL-like channels in its cell membrane (15). In addition to MS channels, this organism has many mechanisms that allow it to sense and react to its environment and obtain the nutrients it requires for growth. Among these mechanisms are three transporters that depend on sodium ions for activity and allow *S. pomeroyi* to adapt to hyperosmotic environments with high salt concentration (41,42). Given that MscCG, an MscS-like channel from *C. glutamicum*, was recently shown to play a role under both hypo- and hyperosmotic conditions in this soil bacterium (35), it is interesting to speculate that MscSP could play a similar role in *S. pomeroyi*. Like MscCG, it could contribute to fine-tuning of the steady-state accumulation of osmolytes in adaptation to hyperosmotic challenge.

We thank Dr. Shaista Shaikh for assistance with the illustrations.

This study was supported by the Australian Research Council (DP0769983), the National Health and Medical Research Council of Australia (635525), and the National Institutes of Health (U54GM094625).

## REFERENCES

1. Martinac, B., M. Buechner, …, C. Kung. 1987. Pressure-sensitive ion channel in Escherichia coli. *Proc. Natl. Acad. Sci. USA.* 84:2297–2301.
2. Levina, N., S. Tötemeyer, …, I. R. Booth. 1999. Protection of Escherichia coli cells against extreme turgor by activation of MscS and MscL mechanosensitive channels: identification of genes required for MscS activity. *EMBO J.* 18:1730–1737.
3. Martinac, B., and A. Kloda. 2003. Evolutionary origins of mechanosensitive ion channels. *Prog. Biophys. Mol. Biol.* 82:11–24.
4. Pivetti, C. D., M. R. Yen, …, M. H. Saier, Jr. 2003. Two families of mechanosensitive channel proteins. *Microbiol. Mol. Biol. Rev.* 67:66–85, table of contents.
5. Koprowski, P., and A. Kubalski. 2003. C termini of the Escherichia coli mechanosensitive ion channel (MscS) move apart upon the channel opening. *J. Biol. Chem.* 278:11237–11245.
6. Bass, R. B., P. Strop, …, D. C. Rees. 2002. Crystal structure of Escherichia coli MscS, a voltage-modulated and mechanosensitive channel. *Science.* 298:1582–1587.
7. Steinbacher, S., R. Bass, …, D. C. Rees. 2007. Structures of the prokaryotic mechanosensitive channels MscL and MscS. *In* Mechanosensitive Ion Channels, Part A. O. P. Hamill, editor. Academic Press, New York. 1–24.
8. Sukharev, S. 2002. Purification of the small mechanosensitive channel of Escherichia coli (MscS): the subunit structure, conduction, and gating characteristics in liposomes. *Biophys. J.* 83:290–298.
9. Anishkin, A., and S. Sukharev. 2004. Water dynamics and dewetting transitions in the small mechanosensitive channel MscS. *Biophys. J.* 86:2883–2895.
10. Nomura, T., M. Sokabe, and K. Yoshimura. 2006. Lipid-protein interaction of the MscS mechanosensitive channel examined by scanning mutagenesis. *Biophys. J.* 91:2874–2881.
11. Vásquez, V., M. Sotomayor, …, E. Perozo. 2008. A structural mechanism for MscS gating in lipid bilayers. *Science.* 321:1210–1214.
12. Martinac, B. 2011. Bacterial mechanosensitive channels as a paradigm for mechanosensory transduction. *Cell. Physiol. Biochem.* 28:1051–1060.
13. Naismith, J. H., and I. R. Booth. 2012. Bacterial mechanosensitive channels–MscS: evolution's solution to creating sensitivity in function. *Annu. Rev. Biophys.* 41:157–177.
14. Börngen, K., A. R. Battle, …, R. Krämer. 2010. Significance of the Corynebacterium glutamicum YggB protein in fine-tuning of compatible solute accumulation. *Biophys. J.* 98:327.
15. Hammon, J., D. V. Palanivelu, …, D. L. Minor, Jr. 2009. A green fluorescent protein screen for identification of well-expressed membrane proteins from a cohort of extremophilic organisms. *Protein Sci.* 18:121–133.
16. Haswell, E. S. 2007. MscS-like proteins in plants. *In* Mechanosensitive Ion Channels, Part A. O. P. Hamill, editor. Academic Press, New York. 329–359.
17. Häse, C. C., A. C. Le Dain, and B. Martinac. 1995. Purification and functional reconstitution of the recombinant large mechanosensitive ion channel (MscL) of Escherichia coli. *J. Biol. Chem.* 270:18329–18334.
18. Battle, A. R., and B. Martinac. 2009. Rapid and efficient co-reconstitution of bacterial mechanosensitive ion channels of small and large conductance into liposomes. *Biophys. J.* 96:256.
19. Nomura, T., C. G. Cranfield, …, B. Martinac. 2012. Differential effects of lipids and lyso-lipids on the mechanosensitivity of the mechanosensitive channels MscL and MscS. *Proc. Natl. Acad. Sci. USA.* 109:8770–8775.
20. Nicholas, K. B., H. B. Nicholas, Jr., and D. W. Deerfield, II. 1997. GeneDoc: analysis and visualization of genetic variation. *EMBNEW. NEWS.* 4:14.
21. Wang, W., S. S. Black, …, I. R. Booth. 2008. The structure of an open form of an E. coli mechanosensitive channel at 3.45 Å resolution. *Science.* 321:1179–1183.
22. Martinac, B., P. R. Rohde, …, A. Kloda. 2010. Studying mechanosensitive ion channels using liposomes. *Methods Mol. Biol.* 606:31–53.
23. Hamill, O. P., and B. Martinac. 2001. Molecular basis of mechanotransduction in living cells. *Physiol. Rev.* 81:685–740.
24. Sukharev, S. I., P. Blount, …, C. Kung. 1994. Functional reconstitution as an assay for biochemical isolation of channel proteins: application to the molecular identification of a bacterial mechanosensitive channel. *Methods.* 6:51–59.
25. Sukharev, S. I., P. Blount, …, C. Kung. 1994. A large-conductance mechanosensitive channel in E. coli encoded by mscL alone. *Nature.* 368:265–268.

26. Berrier, C., M. Besnard, …, A. Ghazi. 1996. Multiple mechanosensitive ion channels from Escherichia coli, activated at different thresholds of applied pressure. *J. Membr. Biol.* 151:175–187.

27. Martinac, B., Y. Saimi, and C. Kung. 2008. Ion channels in microbes. *Physiol. Rev.* 88:1449–1490.

28. Akitake, B., A. Anishkin, and S. Sukharev. 2005. The "dashpot" mechanism of stretch-dependent gating in MscS. *J. Gen. Physiol.* 125:143–154.

29. Akitake, B., R. E. Spelbrink, …, S. Sukharev. 2007. 2,2,2-Trifluoroethanol changes the transition kinetics and subunit interactions in the small bacterial mechanosensitive channel MscS. *Biophys. J.* 92: 2771–2784.

30. Kloda, A., and B. Martinac. 2001. Structural and functional differences between two homologous mechanosensitive channels of Methanococcus jannaschii. *EMBO J.* 20:1888–1896.

31. Sukharev, S. I., B. Martinac, …, C. Kung. 1993. Two types of mechanosensitive channels in the Escherichia coli cell envelope: solubilization and functional reconstitution. *Biophys. J.* 65:177–183.

32. Maksaev, G., and E. S. Haswell. 2012. MscS-like10 is a stretch-activated ion channel from Arabidopsis thaliana with a preference for anions. *Proc. Natl. Acad. Sci. USA.* 109:19015–19020.

33. Sotomayor, M., V. Vásquez, …, K. Schulten. 2007. Ion conduction through MscS as determined by electrophysiology and simulation. *Biophys. J.* 92:886–902.

34. Cox, C. D., A. K. Campbell, …, B. Martinac. 2013. A mechanosensitive channel (MscS) with multiple conducting states shows stronger selectivity for anions in the presence of divalent cations. *Biophys. J.* 102:123.

35. Börngen, K., A. R. Battle, …, R. Krämer. 2010. The properties and contribution of the Corynebacterium glutamicum MscS variant to fine-tuning of osmotic adaptation. *Biochim. Biophys. Acta.* 798: 2141–2149.

36. Reference deleted in proof.

37. Koprowski, P., W. Grajkowski, …, A. Kubalski. 2011. Genetic screen for potassium leaky small mechanosensitive channels (MscS) in Escherichia coli: recognition of cytoplasmic β domain as a new gating element. *J. Biol. Chem.* 286:877–888.

38. Booth, I. R., and P. Blount. 2012. Microbial emergency release valves: the MscS and MscL families of mechanosensitive channels. *J. Bacteriol.* 194:4802–4809.

39. Sukharev, S. I., W. J. Sigurdson, …, F. Sachs. 1999. Energetic and spatial parameters for gating of the bacterial large conductance mechanosensitive channel, MscL. *J. Gen. Physiol.* 113:525–540.

40. Nakamaru, Y., Y. Takahashi, …, T. Nakamura. 1999. Mechanosensitive channel functions to alleviate the cell lysis of marine bacterium, Vibrio alginolyticus, by osmotic downshock. *FEBS Lett.* 444:170–172.

41. Moran, M. A., R. Belas, …, A. Buchan. 2007. Ecological genomics of marine Roseobacters. *Appl. Environ. Microbiol.* 73:4559–4569.

42. Moran, M. A., A. Buchan, …, N. Ward. 2004. Genome sequence of Silicibacter pomeroyi reveals adaptations to the marine environment. *Nature.* 432:910–913.